

## Chapter 2

# Visual Sensing Systems for Arc Welding Process

**Abstract** Visual sensing technology is widely used in welding practices because visual devices are decreasing in price, increasing in reliability and improving in image processing hardware and software. As the most studied welding sensor, CCD (Charge Coupled Device) is more suitable for quality control of welding process than other means of sensing devices because it can obtain both two dimensional and three dimensional information of weld pool, which directly reflect the welding dynamics of molten metal. In this chapter, according to the analysis of arc spectrum and radiation of different materials, visual sensing systems with filters are described. Based on the filtering method, clear images of weld pool are obtained during pulsed GTAW.

The first step of intelligentized arc welding is to imitate the visual system of a welder to extract weld pool size. Passive visual sensing technology has seen great progress in the past years for the abundant information it extracts. Brzakovic et al. [1] obtained the weld pool image in two directions and extracted its geometry information. Wang et al. [2] attempted to get aluminium alloy image for the first time, but it is not clear enough. Zhao et al. [3] developed a passive three-dimension visual sensing method through monocular image which is processed by Shape from Shadow (SFS) algorithm to get the three-dimension geometry of the pool. In this chapter, passive visual sensing system for both aluminium alloy and low carbon steel will be discussed.

### 2.1 Description of the Real-Time Control Systems with Visual Sensing of Weld Pool for the Pulsed GTAW Process

As one of the dominant arc weld methods, pulsed GTAW is widely used in the high-quality weld manufacturing, especially for high-precise thin sheet. High-quality pulsed GTAW requires precise penetration and fine formation of the weld seam, thus real-time regulation of the welding process, i.e., regulating weld pool size, is necessary. Main influences on weld pool size involve electrical conditions, such as pulse duty ratio, peak current, base current, arc voltage, and welding speed; workpiece conditions such as the root opening or geometry of the groove, material, thickness,

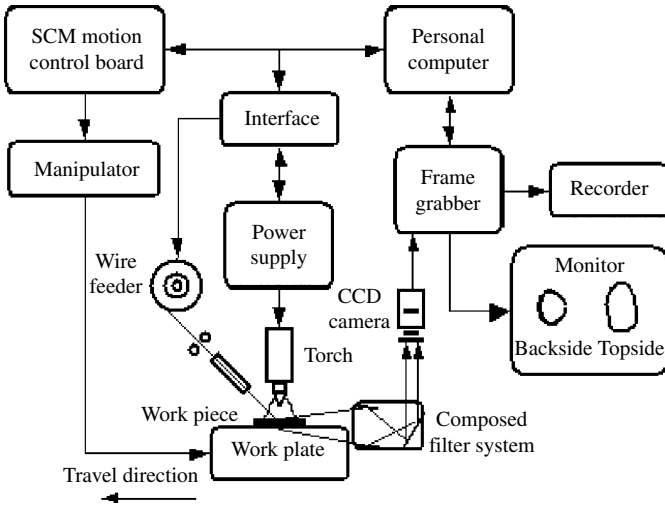


**Fig. 2.1** The structure diagram of experimental system for pulsed GTAW

work piece size, electrode tip angle, and rate of shielding gas flow; welding conditions such as heat transfer condition, arc emission and so on.

The welding experiment is carried out with the monitoring system, which consists of filter system, CCD camera, recorder, frame grabber, and monitor, as shown in Fig. 2.1. The equipment is shown in Fig. 2.2.

The sensing system consists of the following parts as shown in Fig. 2.3(a):

- (1) Light path of double-side imaging simultaneously in a frame. The light path is composed of topside and backside imaging light path. As shown in Fig. 2.3(b), the light from the weld pool reaches the reflector  $O_1$  with the reverse X axis,

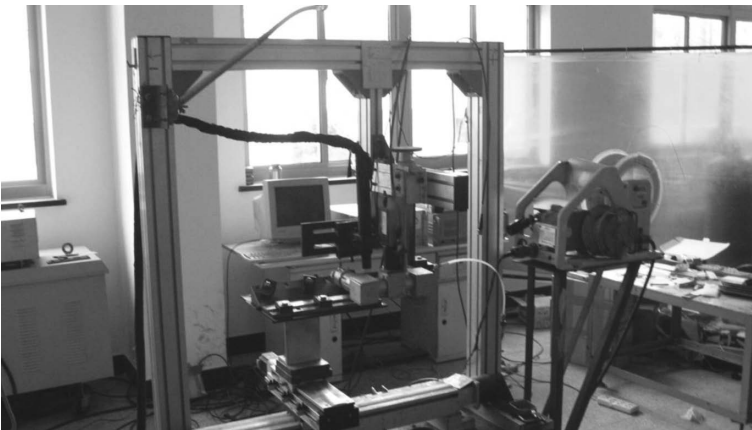


**Fig. 2.2** The photograph of experimental equipment

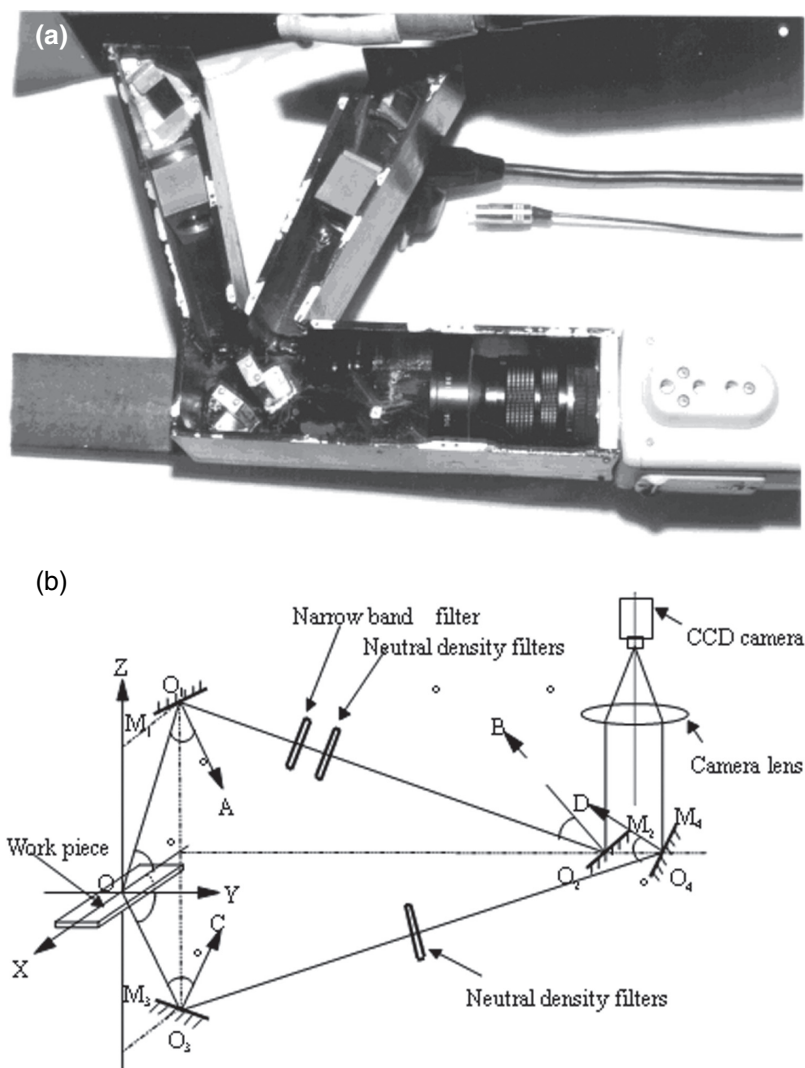


**Fig. 2.3** The sensing system (a) the photograph of sensing system (b) The light path

which is reflected to pass composite filters, then reflected by  $O_2$ , finally focused on the target of the CCD camera. The principle of the backside light path is the same. The light path system is mounted behind the weld pool with a large distance from weld pool to eliminate the pollution from spatter, fume and smoke.

- (2) CCD photograph system transferring the optical signal to video signal. The photograph system includes CCD camera and optical lens.
- (3) Video recorder and monitor system. This subsystem includes V512B frame grabber, recorder and monitor.

## **2.2 The Visual Sensing System and Images of Weld Pool During Low Carbon Steel Pulsed GTAW**

Up to now, most of the researches in the open literatures are on low carbon steel. This is due to good welding quality of the low carbon steel, such as proper heat dissemination, less sensitive to welding parameters, steady chemical capability and weldability compared with other materials.

### ***2.2.1 Analysis of the Sensing Conditions for Low Carbon Steel***

Due to high intensity of arc emission, the weld pool image is strongly interfered. The main task of sensor design is to eliminate the arc interference and to improve the contrast degree of the images. In this book, various visual sensing systems based on the principle of arc emission illumination on the weld pool are discussed.

The arc emission is very complex including continuous spectrum with low intensity and line spectrum with high intensity (consists of metal line, Ar atom, and Ar ion spectrum). The radiance of metal line spectrum is much weaker than that of the continuous arc spectrum, thus not suitable for image capturing. The reflection and diffusion of arc light, therefore, are suitable for image capturing because the concave weld pool serves as a good mirror to send the light into CCD camera. Using this light, the image is with strong intensity and clear weld pool edges.

The intensity of spectral distribution of GTAW with low carbon steel anode is shown in Fig. 2.4 (A). In the range of 600–700 nm there is main continuous spectrum, with few kinds of line spectrum. Figure 2.4 (B) shows the radiation flux under the same conditions. We can see the radiation flux in the range of 600–700 nm is low and flat suitable for light eliminating control.

### ***2.2.2 Capturing Simultaneous Images of Weld Pool in a Frame from Two Directions***

The backside image of weld piece is not available in many practical cases. According to the experience of skilled welder, the geometry of weld pool in both top-side and backside can provide instantaneous information about welding penetration. Topside and backside images of weld pool are needed to be captured and their size characteristics extracted for modeling and controlling of the dynamic welding process. Therefore, a double-side visual sensor is discussed to detect both top and back of the work piece. The sensing system consists of topside and backside light path and composite filters. The schematic diagram of the sensing system is shown in Fig. 2.5.

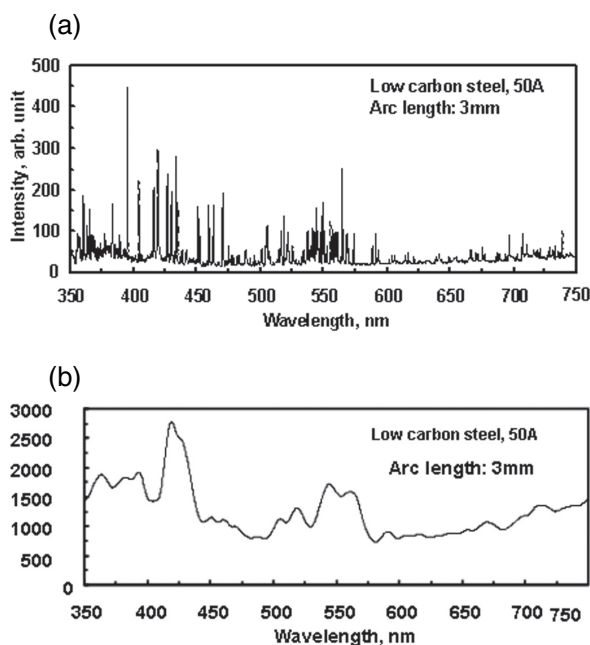


Fig. 2.4 Arc light radiation of GTAW with mild steel anode. (a) The spectral distribution (b) arc light radiation flux

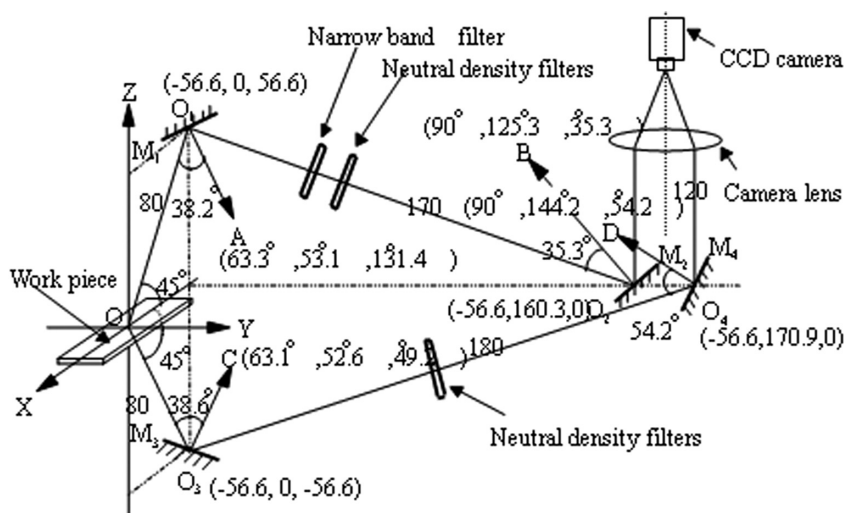


Fig. 2.5 The light path of simultaneous double-side visual image sensing system of weld pool in a frame

In Fig. 2.5, O\_XYZ is work piece coordinate; point O is the center point of the weld pool image. M<sub>1</sub>, M<sub>2</sub>, M<sub>3</sub>, M<sub>4</sub> are reflectors, the centers of which are O<sub>1</sub>, O<sub>2</sub>, O<sub>3</sub> and O<sub>4</sub>. O<sub>1</sub>A, O<sub>2</sub>B, O<sub>3</sub>C and O<sub>4</sub>D represent the normal line of the reflectors respectively, denoted as the angles with each single axis in the coordinate system.

In the previous studies [4–6], the narrowband filtering light system is established to pitch on a center wavelength of the arc spectrum. For low carbon steel, its spectrum intensity is greater than radiant intensity of continuous spectrum adjacent to this metal spectrum line, so that the arc light of other wavelength can be filtered by the selected filter for imaging from self-radiation of weld pool. This kind of filter is feasible to the low carbon steel weld pool due to its distinct contrast between radiation spectrum of the melting metal in weld pool and radiation or reflected spectrum of solid metal on the edge of the weld pool. The composite filter system includes topside and backside light path with different filter. The topside image of weld pool is formed by the illumination from arc emission in the spectral window of 600–700 nm. Topside light path consists of a neural density filter (2 mm depth, and the speed of lens is 1%) and a narrow band filter (the center band is 661 nm, half width is 10 nm, and the peak speed of lens is 28.8%). Backside image is formed by the radiance of the backside metal with high temperature. Two neutral density filters are used in the backside light path with speed of lens of 10% and 50%. Both the topside and backside images concentrate on the same target of the CCD camera through the above double-side imaging light path system.

The system includes CCD camera and optical lens. The focal distance of the lens is 500 nm. The sensitivity of the camera is 0.4 Lux, the area of target is 5.24 × 6.4, and the shutter is set at 1/1000s.

(1) Welding process without wire filler

The experiment conditions for GTAW without wire filler are shown in Table 2.1. Peak current is set at 120 ampere, welding velocity is 2.5 mm/s [7]. A complete weld pool image in a frame is shown in Fig. 2.6, where the left is backside image and the right is the topside image. The image contrast is high, for the nozzle, arc center, topside molten portion, and topside solidified portion can be clearly seen in the topside image. The bright arc around the weld pool is effectively eliminated, and the shape of the tungsten tip emerged from the background. Backside weld pool image is also distinguished from the background.

Figure 2.7 shows top/backside pool serial images in a pulsed cycle. Figure 2.8 (b),(c),(d) are pool images in pulsed peak current and (e),(f),(g) in the pulsed based

**Table 2.1** Experimental conditions of pulsed GTAW

DWP	Pulse frequency	Pulse duty ratio	Base current	Electrode diameter	Angle of tip	Arc length	Flow rate	Specimen size
Unit	f(Hz)	δ(%)	Ib (A)	φ(mm)	θ(°)	l(mm)	L(l/min)	mm×mm×mm
Value	1	45	60	3.2	30	3.5	8.0	280×50×2

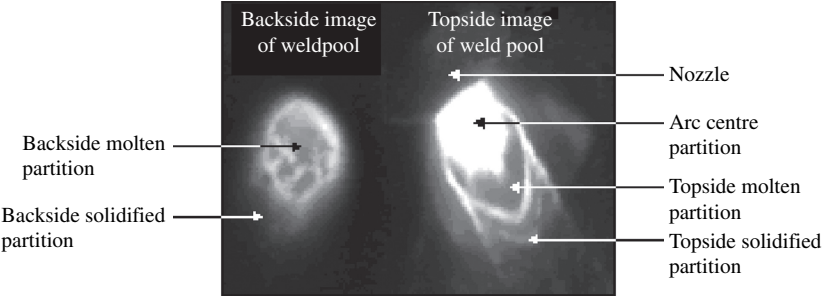


Fig. 2.6 A frame complete weld pool image of pulsed GTAW

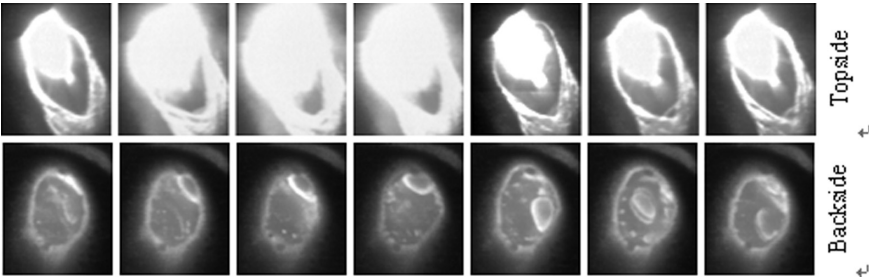


Fig. 2.7 The visual images of the weld pool in different time of a pulse cycle

current. The image is captured under the current of 60 A at 80 ms for a frame complete weld pool image.

The contrast between light reflected from the molten metal surface and that from solid metal surface is distinct; the disturbance can be turned into an advantage for taking a clear image of weld pool.

(2) Welding process with wire filler

The use of wire filler will lead to many changes in the weld pool images, including larger welding current, darker images with blurred weld pool edges. Therefore, a new design of welding experiment parameters is necessary for the welding process with wire filler [8]. Figure 2.8 shows the welding images captured in different period of a pulse.  $T_0$  is at the peak time of the pulse,  $T_1$  is 40 ms after the peak time,  $T_2$  is 100 ms after peak time,  $T_3$  is 200 ms after peak time. It can be inferred from the images that at  $T_0$ , the image is too bright to be dealt with; due to the speed limitation of current regulation, image remain bright at  $T_1$ ; at  $T_2$ , the current is 30 A and the image is clear enough for weld pool edge identification.; At  $T_3$ , however, the image again get blurred. Therefore, the best time for image capturing is 100 ms after peak time.

Under the supposed experiment conditions, welding parameters are set as follows: pulse peak current 120 A, base current 60 A, pulse duty ratio 40%, and welding velocity 2.5 mm/s. According to imaging principle, image is determined by light

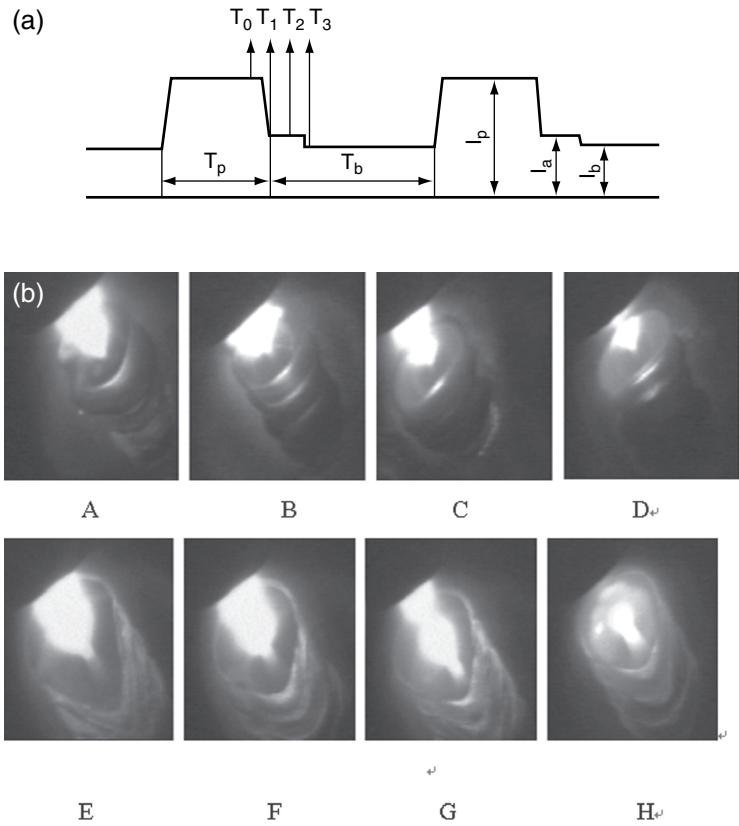


**Fig. 2.8** Influence on the weld pool image during different imaging time (a) time sequence (b) weld pool images; A – 60 A, convex; B – 50 A, convex; C – 40 A, convex; D – 30 A, convex; E – 60 A, concave; F – 50 A, concave; G – 40 A, concave; H – 30 A, concave

source, camera and object shape. Here, imaging current is set as 30 A, and the light source of arc can be supposed as a point light source. The shutter of CCD camera is set as 1/1000s, and the iris diaphragm and filter ratio are fixed.

In Fig. 2.9, when the weld pool is partially penetrating, the top shape of weld pool is approximate to an ellipse, i.e., a convex model image; while on full penetrating, the pool image is similar to a peach shape, i.e. a concave model. The length and stem shape varieties of the weld pool are most obvious.

Due to the impact of arc plasma, the surface of the weld pool depressed in full penetration, while the surface of the weld pool can be convex in partial penetration or with wire filler. The rear part of the weld pool shows the different concave or convex shape distinguishably, as shown in Fig. 2.9.

With the imaging current decreasing, different images of the weld pool are shown in Fig. 2.8 (b–d) and (f–h). It shows that with the imaging current decreasing, the shape of the arc center get concave, and the weld pool gets brighter. And under



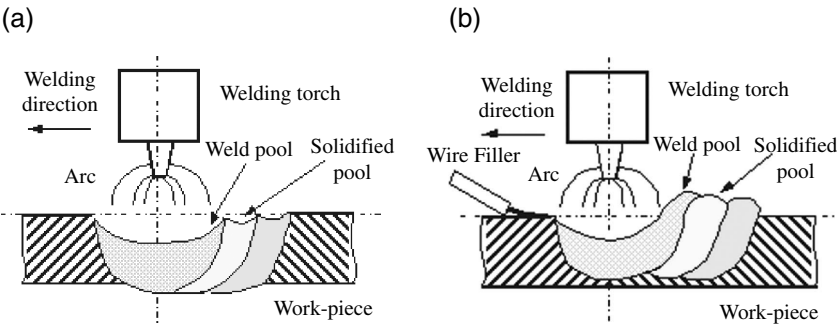


Fig. 2.9 Definition for different type of the weld pool surface (a) Concave type (b) Convex type

imaging current of 30 A, both images of the concave or convex weld pool are clear enough for image processing. The weld pool, the solidified metal, the inverted image of the arc center, and the nozzle of the torch are clearly seen.

2.2.3 Capturing Simultaneous Images of Weld Pool in a Frame from Three Directions

The addition of one light path can offer more visual information. And here the control system includes a double-side visual sensing system from 3 directions, the top-side front, rear, and the backside of weld pool. The light path of the visual system is shown in Fig. 2.10.

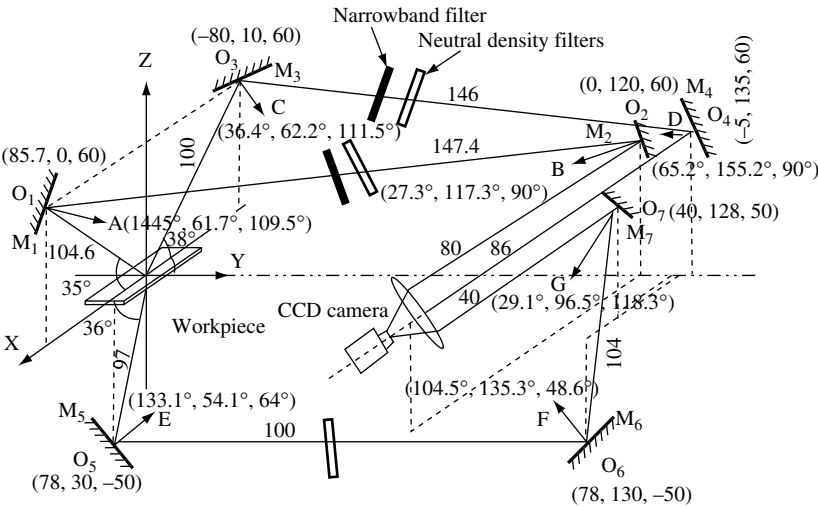
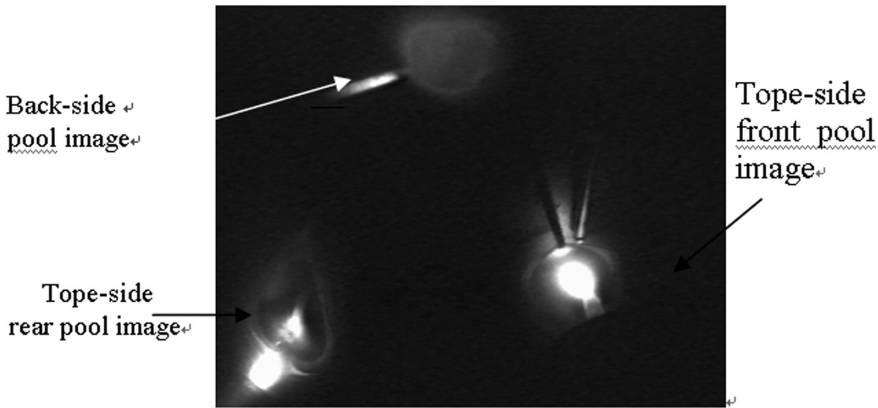


Fig. 2.10 The light path of simultaneous visual imaging system of weld pool in a frame



**Fig. 2.11** A frame complete weld pool image of pulsed GTAW

A complete weld pool images in a frame are shown in Fig. 2.11. And Fig. 2.12 shows the image in different periods.

### **2.3 The Visual Sensing System and Images of Weld Pool During Aluminium Alloy Pulsed GTAW**

Up to now, most of the researches on GTAW sensing systems are for steel plate. Owing to the special features of aluminium alloy welding, such as heat disseminating rapidness, strong oxygenation, evident effects of accumulating heat during welding process, weld seam cutting phenomena, non-distinctive changes in color and luster between melting weld pool and solidified metal region of aluminium alloy, etc., it gets very difficult to control stability and shaped quality of aluminium alloy welding [9, 10]. Since aluminium alloy welding is necessary techniques in aviation, spaceflight and automobile industry, real-time sensing and control of this process is becoming a pressing and challenging technology with development of welding automation.

The sensing system of aluminium alloy welding will be discussed in detail on aluminium alloy arc spectrum analysis, wideband filter design and visual sensing systems construction and image capturing for weld pool.

#### ***2.3.1 Analysis of the Sensing Conditions for Aluminium Alloy***

In contrast with the low carbon steel weld pool, aluminium alloy weld pool has non-distinctive changes in color and luster between melting and solid states, which results in blurred images because radiating spectrums of not only melting pool but

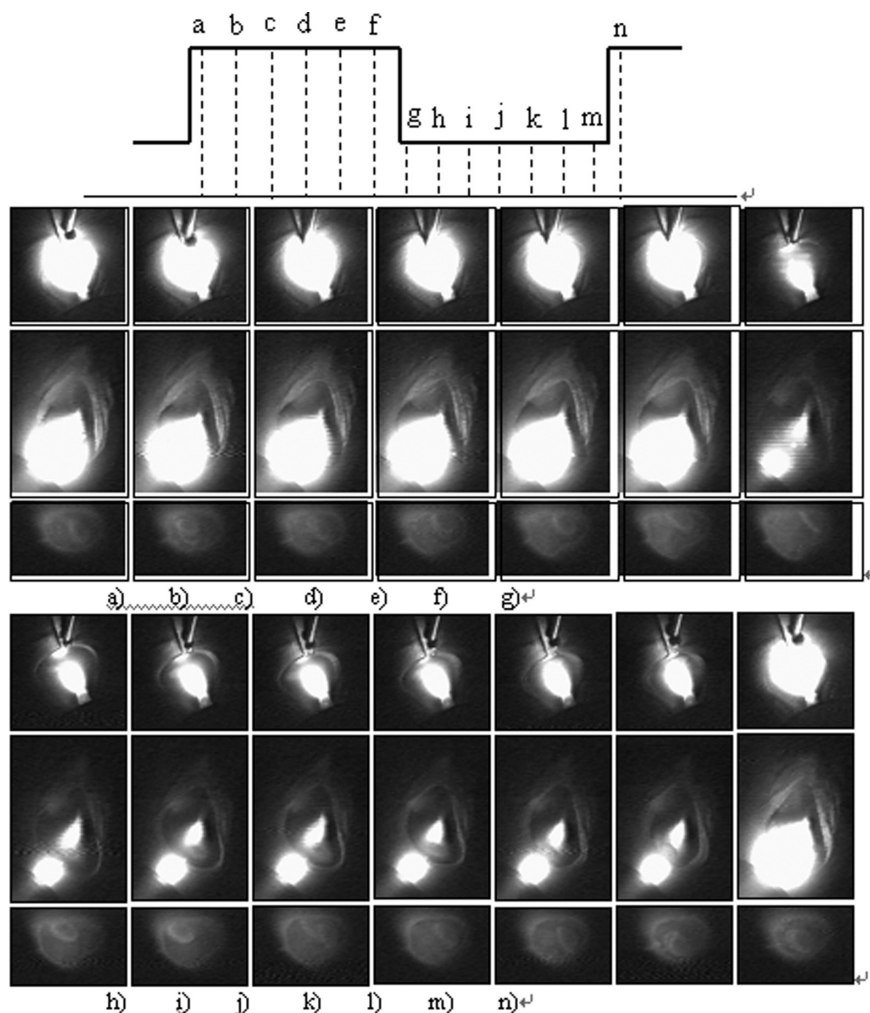


**Fig. 2.12** The weld pool images of different time in a pulse

also of reflecting arc from solid metal surface around the pool exist after narrow filtering. In addition, the narrowband filter also results in a blurred image due to the metal steam on the surface of aluminium alloy weld pool.

Experiments [10] showed that arc spectrum distribution of aluminium alloy GTAW process is composed of both lower intensity continuous spectrum and other different intensity spectrum lines, therefore, it will vary with different technical parameters, e.g., welding current, voltage, materials, etc.. The arc spectrum near the surface region of aluminium alloy weld pool is mainly composed of Al atom spectrum, Al ion spectrum and continuous spectrum radiating from metal black body of the weld pool. The spectrum in the arc pole region includes the spectrum lines of

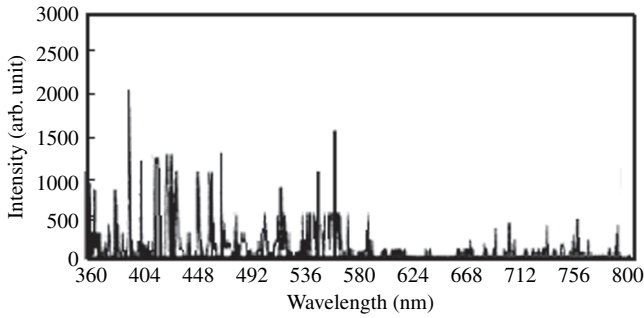


**Fig. 2.13** The distribution of characteristic spectrum of  $A_r$

argon atom, ion and other metal steam. The distributions of atomic and ion spectrum lines of argon and Al under blazing condition in arc welding process are shown as Figs. 2.13 and 2.14. The Figures indicate that within the visible light spectrum band of 380–760 nm, the density of Al spectrum is stronger than that of argon only when the wavelength is 396 nm.

If using the narrowband filter in the center wavelength 396–560 nm, aluminium alloy spectrum lines would be submerged in the spectrums of argon. Moreover, welding current variation will result in intensity changes of discrete spectrum lines and pollution of weld pool images, and common CCD camera is less sensitive to visible light. Experiments [10] also show that the narrowband filter used for low carbon weld pool is unsuitable to capture clear weld pool image during aluminium alloy pulsed GTAW process.

However, in the near infrared band 580–720 nm, according to the spectrum distributions in Figs. 2.13 and 2.14, the spectrum lines of argon and other metal and nonmetals are relatively weak compared with those of aluminium alloy, because the spectrum lines of aluminium alloy are continuous, while almost no argon spectrum line is distributed in 640–670 nm band. Moreover, in the case of welding current more than 80 A, the intensity of continuous spectrum in the near infrared band keeps stable even when welding current had a fluctuation of  $\pm 20$  A. Therefore, using

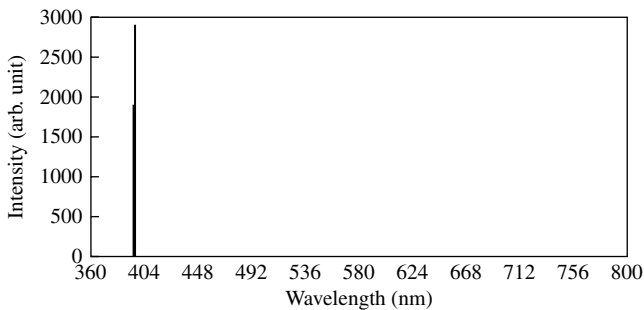


**Fig. 2.14** The distribution of characteristic spectrum of aluminium alloy

the arc continuous spectrum in the near infrared band for illuminating aluminium alloy welding pool would greatly decrease interferences from other various spectrum lines.

According to the above characteristics of aluminium alloy weld pool, a wideband filtering method is presented and the filtering system is established to enlarge permeating light range of the filter and to improve anti-interference ability of the visual sensing system by illumination of continuous and discrete spectrum in the wideband and an appropriate reducing light measures. Based on a large number of experiments, the parameters of the wideband filtering system are determined as follows, permeating light range is 590—710 nm, permeating ratio of reducing light lens in the upside light path of the weld pool is 20%, and permeating ratio of reducing light lens in the backside light path of the weld pool is 90%. The response curve of the frequency spectrum of the designed wideband filter is shown as Fig. 2.15. Using the developed wideband filtering system, clear images of aluminium alloy weld pool during pulsed GTAW process can be captured.

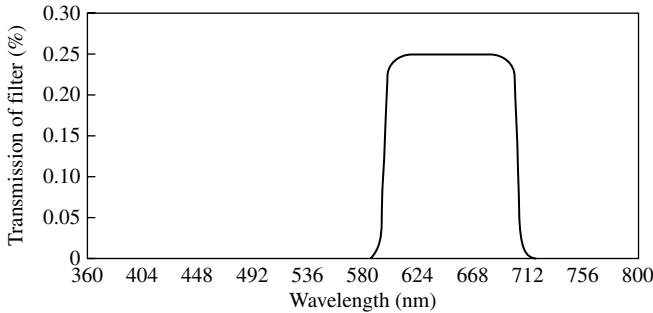


**Fig. 2.15** Response curve of the frequency spectrum of the wideband filter

### 2.3.2 Capturing Simultaneous Images of Weld Pool in a Frame from Two Directions

Combining the analysis of arc spectrum features of aluminium alloy weld pool and the idea of wideband filter, a visual sensing system with topside and backside light paths and composite filters is developed to capture the topside and backside images of the aluminium alloy weld pool simultaneously in the same frame [10].

The system restrains some particular wavelength from passing through the primary filter and can observe the weld pool with the continuous spectrum of the arc light. Based on welding experiment and related result analysis, the parameters of the light filter system are determined as follows: the primary filter is a 560–700 nm glass filter, only the light of wavelength longer than 560 nm or shorter than 700 nm can pass through it, so it filters out the high intense noise of argon's and etc. An attenuation of the dimmer glass is 30%. Depth of field is 1/1000, and the shutter is

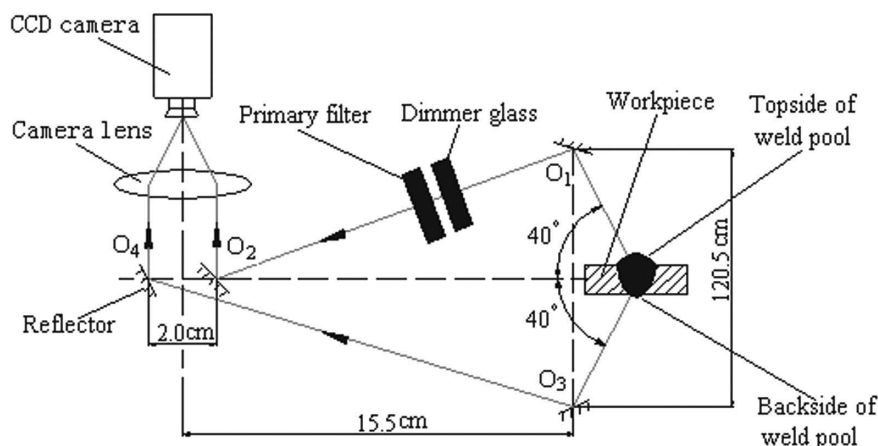


**Fig. 2.16** Light path structure of double-side sensing systems for Al alloy weld pool

set at  $1/125$  s. The function of reducing light is realized by the dimmer glass and the CCD camera aperture is adjustable. Figure 2.16 shows a schematic diagram of the double-sided visual sensing system, which contains the topside and backside imaging light paths. The light from the topside weld pool reached the reflector  $O_1$  at an angle of 40-deg with the X-axis, and is reflected through the dimmer glass and primary filter, then reflected  $O_2$ , and finally focused on the target of the CCD camera. The backside light path is shown in the bottom part of Fig. 2.16.

Through investigation of Al welding experiments, the pulse current pattern is designed as Fig. 2.17 for realizing a higher efficiency of welding heat input during the peak time of the pulse level and acquiring of the pool image in the based level. In practical welding, the main aim of control welding process is to ensure a stable welding with desirable appearance.

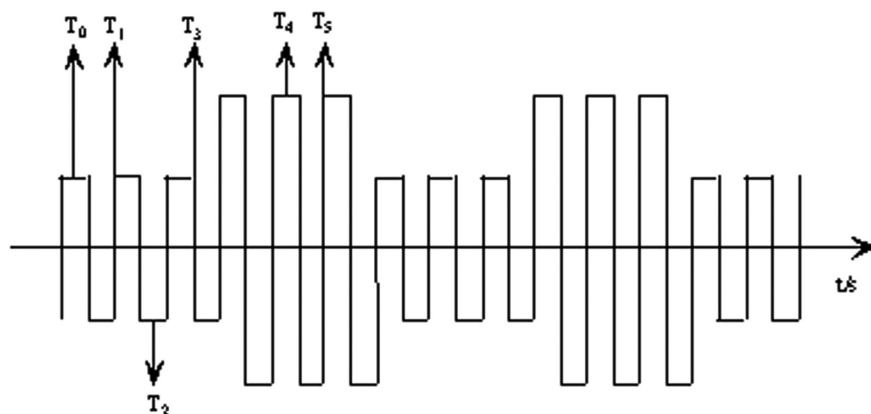


**Fig. 2.17** Pulsed wave of welding current

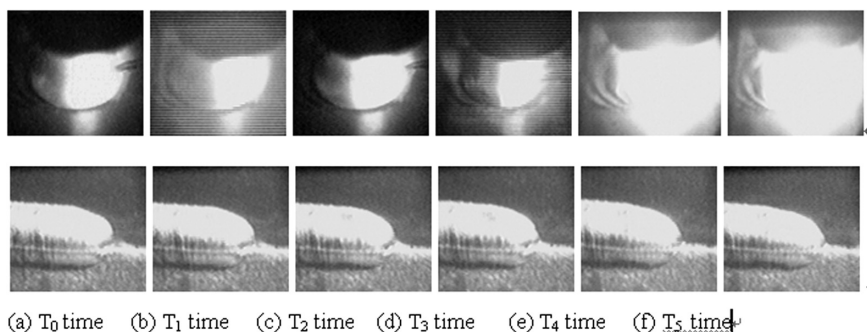


**Fig. 2.18** Images of different time molten pool in a pulse cycle (a)  $T_0$  time (b)  $T_1$  time (c)  $T_2$  time (d)  $T_3$  time (e)  $T_4$  time (f)  $T_5$  time

Because the difference of polarity and intensity in different time pulsed current, image quality of the weld pool depends on different image capturing time. Corresponding to the different time in Fig. 2.18,  $T_0$ ,  $T_1$ , ...  $T_5$ , where  $T_0$  is the based current time at the stable positive polarity,  $T_1$  is the transition time of the based current from negative to positive polarity,  $T_2$  is the based current time at the stable negative polarity,  $T_3$  is the transition time of the based current from positive to negative polarity,  $T_4$  is the peak current time at the stable positive polarity, and  $T_5$  is the transition time of the peak current from negative to positive polarity. The captured images of topside and backside weld pool during Aluminium alloy pulsed GTAW are showed as Fig. 2.18, (a), (b), ... (f). The images in Fig. 2.18 are continuous topside and backside images taking in a pulsed current period, the image (a) is corresponding to  $T_0$  time, the image (b) to  $T_1$ , ... and the image (f) to  $T_5$ .

Under the welding experiment conditions: the frequency of pulse peak current is 2 Hz, the width of pulse peak current is 375 ms, the duration of pulse base current is 125 ms, the main influence on definition of weld pool images is the based current value. In Fig. 2.19, four different based current values at the time A, B, C and D are chosen for comparing the image quality. The images corresponding to base current 70 A at time A, 80 A at time B, 90 A at time C, and 100 A at time D are shown as Fig. 2.20. One can see the evident conclusion as following: if the based current value

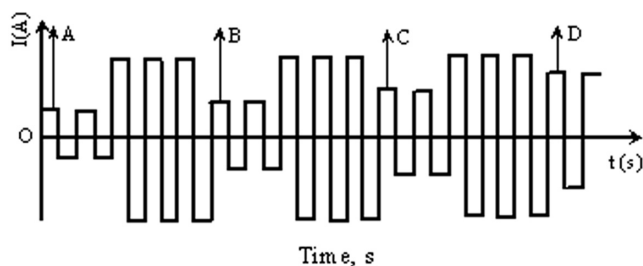


**Fig. 2.19** The different based current

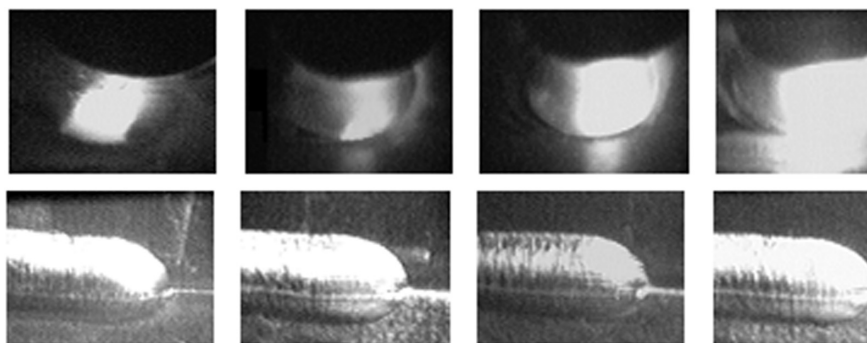


**Fig. 2.20** The aluminium alloy weld pool images of different based current (a) 70 A (b) 80 A (c) 90 A (d) 100 A

is too large or small, i.e. the arc light is too strong or weak, the contrast between the pool region and the background in the image is unclear so that the boundary of weld pool and image characteristic can't be distinguished easily. Comparing with images at different based current values, the 90 A at the C time is selected the proper base current value for taking image of aluminium alloy weld pool.

Based on investigation of the above experiment results, the proper DWP for taking fine images of aluminium alloy weld pool during pulsed GTAW process are designed as Table 2.2 A typical images of the topside and backside weld pool are captured, shown as Fig. 2.21. The profile image of the weld pool is obtained from the direction paralleled to the one in which the welding gun moved. The image of the topside weld pool in Fig. 2.21 can be divided into the following parts: nozzle, deposited area of metal heap, weld brim, base metal, center of weld pool, cathode spot area and arc column etc. The nozzle reflects light least, so the gray level is low and looks black; the cathode spot area is the part whose oxidized film is removed by the arc, its gray level lies between the highest and that of the image background; arc column shines most strongly and it has a high gray level; the molten metal in the front of weld pool also reflects intensely, and is approximately like a mirror, so its gray level is the highest and it looks white. In the rear region of weld pool, the welding wire and base metal are melting and flowing backward, and the metal piles up, which produces a scattered reflectance of the arc and so only the part arc

**Table 2.2** Experimental conditions of pulsed GTAW for aluminium alloy

Pulse frequency $f$ , Hz	2	Traveling speed $V$ , mm/s	3.3
AC frequency $f$ , Hz	50	Arc length $\iota$ , mm	5
Peak current $I_p$ , A	220	Electrode diameter $\phi$ , mm	3
Based current $I_b$ , A	90	Argon flow rate $L$ , l/min	8.0
Wire feed speed $V_f$ , mm/s	15	Workpiece size, mm <sup>3</sup>	250×50×3



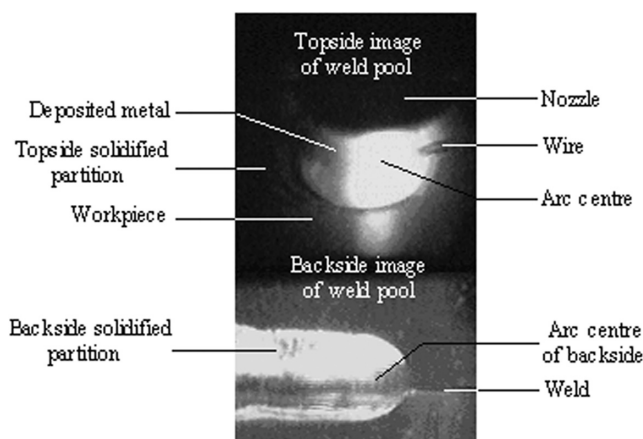


**Fig. 2.21** A frame complete molten pool image of Al alloy in pulsed GTAW

is received by the CCD, and this region has a weaker light. The weld brim is clear and the border of welding seam is clearly observed. The image of the backside weld pool in Fig. 2.21 contains some information of welding direction and weld width.

### ***2.3.3 Capturing Simultaneous Images of Weld Pool in a Frame from Three Directions***

In this part, a visual sensing system of three directions, namely, frontal, rear-upside and backside direction, is presented [11, 12]. In Fig. 2.22(a), the visual sensing subsystem is composed of a CCD camera, lenses and special filters and image processing algorithms. Figure 2.22(b) shows the visual sensor for GTAW pool with three light path. The visual sensor can acquire nearly all information in a frame about the weld pool from three directions at the same time [12].

The Fig. 2.23 shows the structure diagram of visual sensing and control systems with three light paths for aluminum alloy pulse GTAW. And Fig. 2.24 is a photograph of the visual sensing and real-time control experimental systems for the aluminum alloy GTAW.

At basic current, the intensive arc light momentarily extinguishes periodically with short-circuit. The short-circuit phenomena is utilized in order to acquire an image of the weld pool and its vicinity using the vision sensor.

Figure 2.25 is a whole frame image of weld pool from top-back, top-front and back directions. And Fig. 2.26 is the top-front image of the weld pool. Beside welding pool, there are many other parts in the image such as arc, gap, groove and wire.

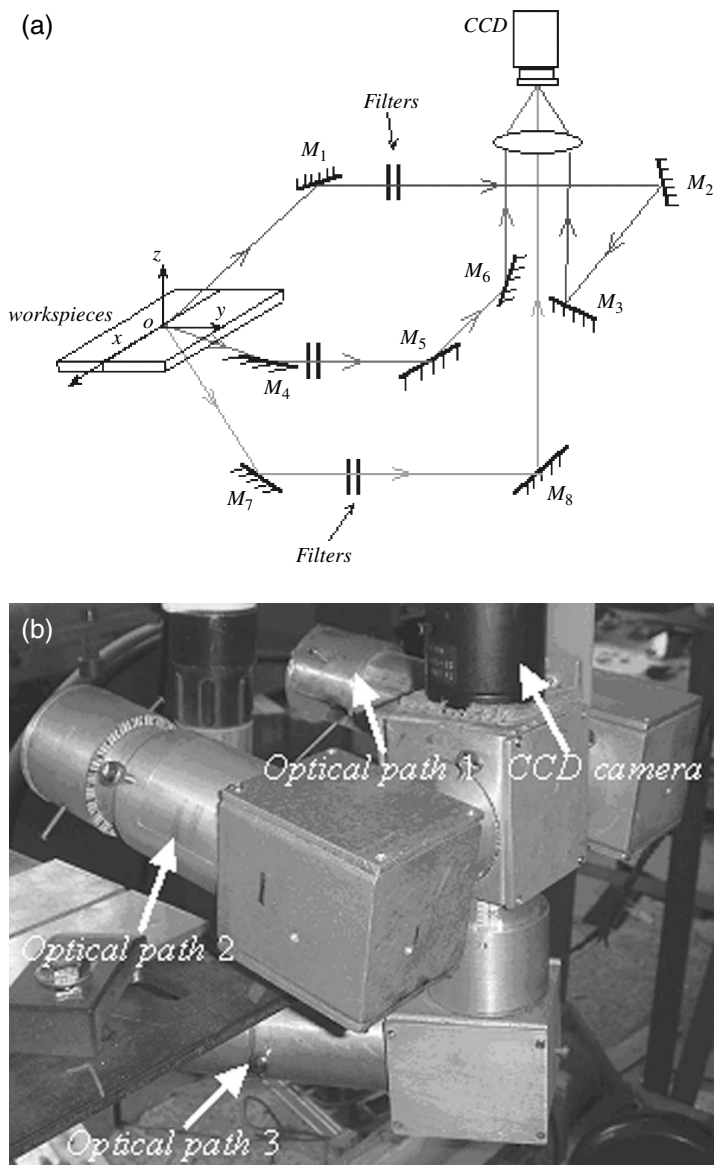


**Fig. 2.22** The visual sensor subsystem (a) Diagram of visual sensing system (b) The visual sensor for GTAW pool with three light paths [12]

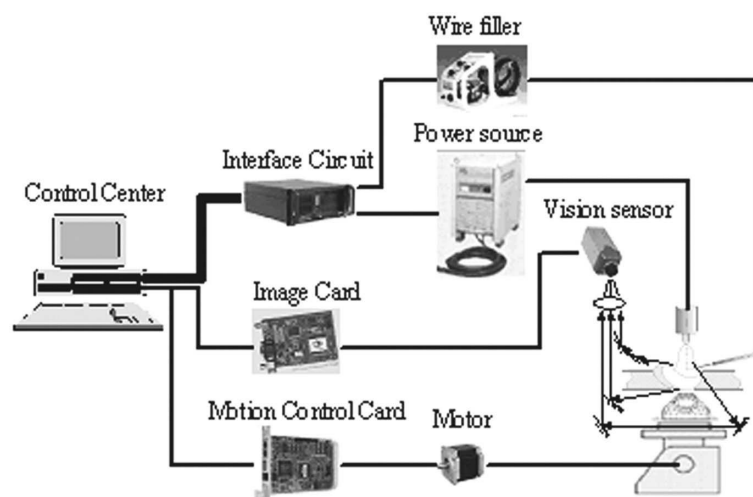


**Fig. 2.23** The structure diagram of visual sensing and control systems for aluminum alloy pulse GTAW [12]

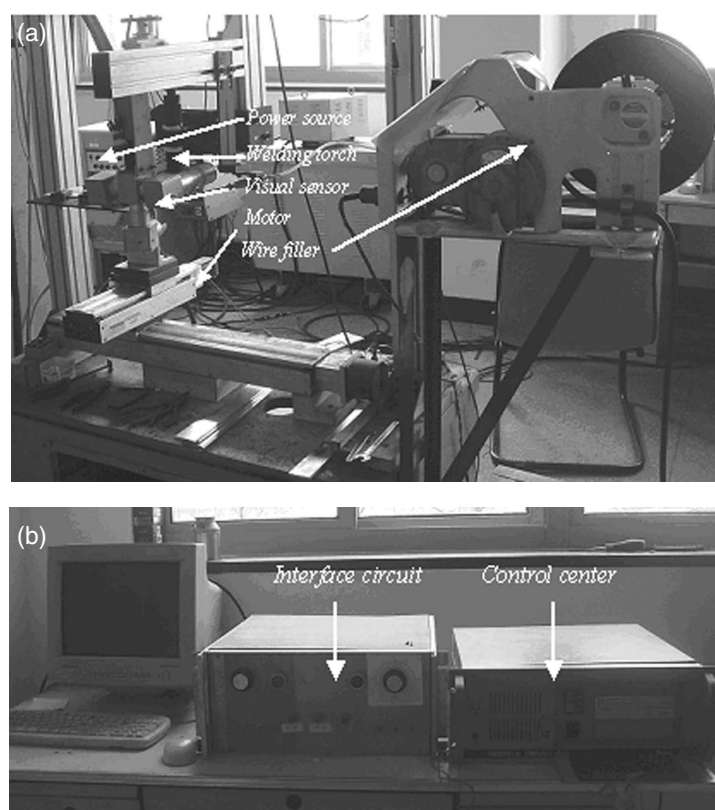


**Fig. 2.24** A photograph of the experimental systems for aluminum alloy GTAW [12] (a) Welding unit (b) Control center

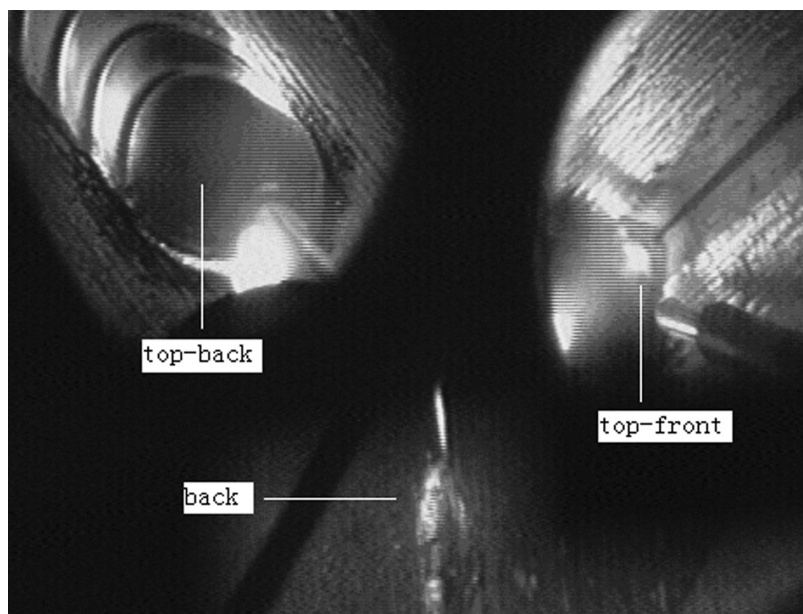
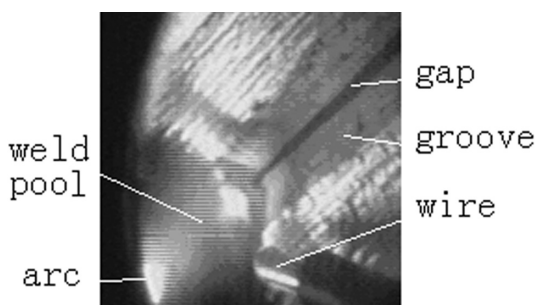


**Fig. 2.25** The three-direction weld pool image

**Fig. 2.26** The top-front part image



## 2.4 The Chapter Conclusion Remarks

According to the analysis of arc spectrum and radiation of low carbon steel and aluminium alloy, visual sensing systems with filters are described. Based on the filtering method, and proper welding parameters, clear images of weld pool are obtained during pulsed GTAW.

## References

1. D. Brzakovic, D.T. Khani, Weld pool edge detection for automated control of welding. *IEEE Transactions on Robotics and Automation*. 1991, 7(3):397–403
2. J.J. Wang, T. Lin, S.B. Chen. Obtaining weld pool vision information during aluminium TIG welding. *International Journal of Advanced Manufacture Technology*, London, UK, 2005, V26:219–227
3. D.B. Zhao, Y.J. Lou, S.B. Chen, L. Wu. Surface height and geometry parameters for describing shape of weld pool during pulsed GTAW. *SPIE International Symposium on Intelligent System and Advanced Manufacturing*, Boston, Massachusetts, USA, 1999, V3833:91–99
4. S.B. Chen, Y.J. Lou, L. Wu, D.B. Zhao. Intelligent methodology for measuring, modeling, control of dynamic process during pulsed GTAW – Part I Bead-on-plate welding. *Welding Journal*. 2000, 79(6):151s–163s
5. S.B. Chen, D.B. Zhao, L. Wu, Y.J. Lou, Intelligent methodology for measuring, modeling, control of dynamic process during pulsed GTAW – Part II butt welding. *Welding Journal*. 2000, 79(6):164s–174s
6. D.B. Zhao, S.B. Chen, L. Wu, Q. Chen. Intelligent control for the double-sided shape of the weld pool in pulsed GTAW with wire filler. *Welding Journal*. 2001, 80(11):253s–260s
7. L. Yajun. “Intelligent Control for Pulsed GTAW Dynamic Process Based on Image Sensing of Weld Pool”, PhD dissertation, Harbin Institute of Technology, 1998
8. D. Zhao. Dynamic Intelligent Control for Weld Pool Shape during Pulsed GTAW with Wire Filler Based on Three-Dimension Visual Sensing, [Doctorial dissertation], Harbin Institute of Technology, 2000
9. Q.L. Wang, C.L. Yang, Z. Geng. Separately excited resonance phenomenon of the weld pool and its application. *Welding Journal*. 1993, 72(9):455–462
10. J.J. Wang, Visual information acquisition and adaptive control of weld pool dynamics of Aluminum alloy during pulsed TIG welding. PhD dissertation, Shanghai Jiao Tong University, 2003
11. C. Fan, F. Lv, S. Chen, 5–8 Nov. 2007, “A visual sensing system for welding control and seam tracking in aluminum alloy gas tungsten arc welding”, *Industrial Electronics Society*, 2007. *IECON 2007. 33rd Annual Conference of the IEEE*, Taipei: 2700–2705
12. C. Fan, Visual densing and intellignet control of varied gap AI alloy pulsed GTAW process, [2.Doctorial dissertation]. Shanghai Jiao Tong University, 2008



Intelligentized Methodology for Arc Welding Dynamical  
Processes

Visual Information Acquiring, Knowledge Modeling and  
Intelligent Control

Chen, S.-B.; Wu, J.

2009, XXIV, 278 p. 502 illus., Hardcover

ISBN: 978-3-540-85641-2